



Year: 2023

7 T MRI of the Cervical Neuroforamen: Assessment of Nerve Root Compression and Dorsal Root Ganglia in Patients With Radiculopathy

Feuerriegel, Georg C ; Marth, Adrian A ; Germann, Christoph ; Wanivenhaus, Florian ; Nanz, Daniel ; Sutter, Reto

Abstract: **OBJECTIVES:** The aim of this study was to assess the diagnostic value of 3-dimensional dual-echo steady-state (DESS) magnetic resonance imaging (MRI) of the cervical spine at 7 T compared with 3 T in patients with cervical radiculopathy. **MATERIALS AND METHODS:** Patients diagnosed with cervical radiculopathy were prospectively recruited between March 2020 and January 2023 before undergoing surgical decompression and received 3-dimensional DESS imaging at 3 T and 7 T MRI. Cervical nerve root compression and the dimensions of the dorsal root ganglia were assessed by 2 radiologists independently. Signal intensity, visibility of nerve anatomy, diagnostic confidence, and image artifacts were evaluated with Likert scales. The degree of neuroforaminal stenosis was assessed on standard clinical 3 T scans. Statistics included the analysis of the diagnostic accuracy and interreader reliability. The Wilcoxon signed rank test was used to assess differences between the groups. **RESULTS:** Forty-eight patients (mean age, 57 ± 12 years; 22 women) were included in the study with the highest prevalence of severe neuroforaminal stenosis observed at C6 ($n = 68$) followed by C7 ($n = 43$). Direct evaluation of nerve root compression showed significantly higher diagnostic confidence and visibility of cervical nerve rootlets, roots, and dorsal root ganglia on 7 T DESS than on 3 T DESS (diagnostic confidence: $P = 0.01$, visibility: $P < 0.01$). Assessment of nerve root compression using 7 T DESS allowed more sensitive grading than standard clinical MRI ($P < 0.01$) and improved the performance in predicting sensory or motor dysfunction (area under the curve combined: 0.87). **CONCLUSIONS:** 7 T DESS imaging allows direct assessment of cervical nerve root compression in patients with radiculopathy, with a better prediction of sensory or motor dysfunction than standard clinical MRI. Diagnostic confidence and image quality of 7 T DESS were superior to 3 T DESS.

DOI: <https://doi.org/10.1097/RLL.0000000000001039>

Posted at the Zurich Open Repository and Archive, University of Zurich

ZORA URL: <https://doi.org/10.5167/uzh-254436>

Journal Article

Published Version



The following work is licensed under a Creative Commons: Attribution-NonCommercial-NoDerivatives 4.0 International (CC BY-NC-ND 4.0) License.

Originally published at:

Feuerriegel, Georg C; Marth, Adrian A; Germann, Christoph; Wanivenhaus, Florian; Nanz, Daniel; Sutter, Reto (2023). 7 T MRI of the Cervical Neuroforamen: Assessment of Nerve Root Compression and Dorsal Root Ganglia in Patients With Radiculopathy. *Investigative Radiology*:Epub ahead of print.

DOI: <https://doi.org/10.1097/RLI.0000000000001039>

7 T MRI of the Cervical Neuroforamen

Assessment of Nerve Root Compression and Dorsal Root Ganglia in Patients With Radiculopathy

Georg C. Feuerriegel, MD, Adrian A. Marth, MD, Christoph Germann, MD, Florian Wanivenhaus, MD, Daniel Nanz, PhD, and Reto Sutter, MD

Objectives: The aim of this study was to assess the diagnostic value of 3-dimensional dual-echo steady-state (DESS) magnetic resonance imaging (MRI) of the cervical spine at 7 T compared with 3 T in patients with cervical radiculopathy.

Materials and Methods: Patients diagnosed with cervical radiculopathy were prospectively recruited between March 2020 and January 2023 before undergoing surgical decompression and received 3-dimensional DESS imaging at 3 T and 7 T MRI. Cervical nerve root compression and the dimensions of the dorsal root ganglia were assessed by 2 radiologists independently. Signal intensity, visibility of nerve anatomy, diagnostic confidence, and image artifacts were evaluated with Likert scales. The degree of neuroforaminal stenosis was assessed on standard clinical 3 T scans. Statistics included the analysis of the diagnostic accuracy and interreader reliability. The Wilcoxon signed rank test was used to assess differences between the groups.

Results: Forty-eight patients (mean age, 57 ± 12 years; 22 women) were included in the study with the highest prevalence of severe neuroforaminal stenosis observed at C6 ($n = 68$) followed by C7 ($n = 43$). Direct evaluation of nerve root compression showed significantly higher diagnostic confidence and visibility of cervical nerve rootlets, roots, and dorsal root ganglia on 7 T DESS than on 3 T DESS (diagnostic confidence: $P = 0.01$, visibility: $P < 0.01$). Assessment of nerve root compression using 7 T DESS allowed more sensitive grading than standard clinical MRI ($P < 0.01$) and improved the performance in predicting sensory or motor dysfunction (area under the curve combined: 0.87).

Conclusions: 7 T DESS imaging allows direct assessment of cervical nerve root compression in patients with radiculopathy, with a better prediction of sensory or motor dysfunction than standard clinical MRI. Diagnostic confidence and image quality of 7 T DESS were superior to 3 T DESS.

Key Words: radiculopathy, magnetic resonance imaging, ganglia

(*Invest Radiol* 2024;00: 00–00)

Received for publication August 21, 2023; and accepted for publication, after revision, September 8, 2023.

From the Department of Radiology, Balgrist University Hospital, Faculty of Medicine, University of Zurich, Zurich, Switzerland (G.C.F., A.A.M., C.G., D.N., and R.S.); Swiss Center for Musculoskeletal Imaging, Balgrist Campus AG, Zurich, Switzerland (A.A.M. and D.N.); and Department of Orthopedic Surgery, Balgrist University Hospital, Faculty of Medicine, University of Zurich, Zurich, Switzerland (F.W.).

Conflicts of interest and sources of funding: none declared.

Correspondence to: Georg C. Feuerriegel, MD, Department of Radiology, Balgrist University Hospital, Faculty of Medicine, University of Zurich, Forchstrasse 340, 8008 Zurich, Switzerland. E-mail: georg.feuerriegel@balgrist.ch.

Supplemental digital contents are available for this article. Direct URL citations appear in the printed text and are provided in the HTML and PDF versions of this article on the journal's Web site (www.investigativeradiology.com).

Copyright © 2023 The Author(s). Published by Wolters Kluwer Health, Inc. This is an open-access article distributed under the terms of the Creative Commons Attribution-Non Commercial-No Derivatives License 4.0 (CCBY-NC-ND), where it is permissible to download and share the work provided it is properly cited. The work cannot be changed in any way or used commercially without permission from the journal.

ISSN: 0020-9996/24/0000-0000

DOI: 10.1097/RLI.0000000000001039

Over the last years, technical advancements of ultra-high field magnetic resonance imaging (MRI) at 7 T have contributed to its development as a valuable tool for musculoskeletal imaging.¹ Compared with 1.5 and 3 T MRI, 7 T MRI provides an increased signal-to-noise ratio, thus increasing spatiotemporal and spectral resolution, which enables better assessment of morphologic, biochemical, and functional details of musculoskeletal tissues.^{2–4} Several studies have assessed different use cases for 7 T MRI in musculoskeletal imaging and found advantages compared with 3 T MRI.^{5–10} Germann et al⁵ recently demonstrated a higher sensitivity of dual-echo steady-state (DESS) knee imaging at 7 T for detecting meniscal and chondral calcifications in patients with calcium pyrophosphate deposition disease. In a study by Riegler et al,¹¹ the authors were able to demonstrate the ability of 7 T MRI to assess the number of axonal bundles in the median nerve of the wrist using a triple-echo steady-state sequence. They also generated normative T2 values of the nerve and observed higher T2 values in patients with idiopathic carpal tunnel syndrome than in healthy volunteers.¹¹

Magnetic resonance imaging is the current imaging standard for the assessment of cervical radiculopathy due to its noninvasive character and excellent soft tissue contrast.¹² Cervical radicular pain is often caused by impingement of the cervical nerves and/or roots due to neuroforaminal stenosis. The stenosis is commonly caused by degenerative changes of the intervertebral disc or facet joints and less commonly by trauma, tumor, or meningeal and synovial cysts.¹³ The degree of stenosis is graded according to Park et al¹⁴ and assesses the amount of perineural fat obliteration around the cervical nerves in sagittal oblique T2-weighted images. However, the anatomy of the cervical nerve roots is complex and delicate, and the spatial resolution of conventional MRI is often not good enough for direct nerve imaging.^{15,16} Novel MRI sequences have been established in recent years including 3-dimensional (3D) DESS imaging in order to increase the sensitivity and specificity for direct nerve visualization.¹⁵ Wang et al¹⁵ compared 3 different MR sequences at 3 T MRI optimized for imaging of cervical nerves and found 3D DESS to allow the best nerve assessment in patients with cervical radiculopathy. Galley et al⁹ recently demonstrated the use of the higher spatial resolution at 7 T for the depiction of cervical nerve rootlets using a 3D DESS sequence. Although not statistically significant, the authors were able to identify a larger number of individual cervical rootlets on 7 T MRI than on 3 T MRI, indicating superior image quality. However, none of the patients presented with a pathology. Therefore, the aim of this study was to assess the diagnostic value of 3D DESS MRI of the cervical nerve rootlets, roots, and dorsal root ganglia (DRG) at 7 T compared with 3 T in patients with cervical radiculopathy.

MATERIALS AND METHODS

Participant Selection

For this study, patients diagnosed with cervical radiculopathy were prospectively recruited between March 2020 and January 2023

TABLE 1. Patient Characteristics, Degree of Neuroforaminal Stenosis, and Sensory or Motor Dysfunction

Age, y*					57 ± 12
Male					26
Female					22
Level	Neuroforaminal Stenosis [†]				Symptoms of Sensory or Motor Dysfunction [‡]
	None	Mild	Moderate	Severe	
C2 (n)	96	0	0	0	0
C3 (n)	86	10	0	0	2
C4 (n)	66	14	7	9	2
C5 (n)	43	22	18	13	12
C6 (n)	16	12	34	34	38
C7 (n)	39	14	20	23	23
C8 (n)	95	3	1	0	2

*Data are given as mean ± standard deviation.

[†]Degree of stenosis assessed according to Park et al.¹⁴

[‡]Assessed by clinical examination and patient anamnesis.

n = number of neuroforamen/ affected nerve roots.

(n = 48; Table 1, Fig. 1) before undergoing surgical decompression. Symptoms included shooting electric pain in the upper limb, neck pain, and pain due to sensory, motor, and/or reflex deficits. Diagnosis was made by spine surgeons, and the main affected nerve root was determined on the basis of symptoms, physical and clinical examination, and the results of a conventional clinical 3 T MRI performed before enrolment. Other examinations, such as electrophysiological tests, were not available at the time of the enrolment. To determine the success of surgical decompression, changes in disability due to cervical radiculopathy were assessed before and 6 months after surgical decompression using the Neck Disability Index (NDI).^{17–19} Patients with a history of cervical spine surgery, tumors, metal implants, or contraindications for MRI (eg, cardiac pacemaker, claustrophobia, pregnancy) were excluded from the present study. Written informed consent was obtained from all study participants before inclusion. Three patients withdrew from participation due to symp-

toms of claustrophobia experienced during conventional MRI. The study protocol was approved by the institutional review board (Cantonal Ethics Committee, Zurich).

Magnetic Resonance Imaging

All patients underwent 3D DESS imaging on a 7 T MR system (Magnetom Terra; Siemens Healthineers) with an 8-channel C-spine surface array transmit-receive coil (Rapid Biomedical GmbH) and a 3 T MR system (Magnetom Prisma; Siemens Healthineers with a 20-channel head/neck receive coil [Siemens Healthineers]). The 3D DESS sequence, which was established in a previous study, was acquired at both field strengths.⁹ Sequence parameters have been optimized for 3 T and 7 T to achieve a high spatial resolution with visually comparable SNR at clinically acceptable and comparable scan times. Detailed scan parameters are listed in Supplementary Table S1, <http://links.lww.com/RLI/A863>.

In addition, all patients received a conventional 3 T MRI before inclusion as part of the routine diagnostic workup. These conventional 3 T images were assessed by 2 radiologists (*blinded for review*) as a consensus measure of the degree of neuroforaminal stenosis according to Park et al¹⁴ and used as a reference standard. Detailed scan parameters are listed in Supplementary Table S2, <http://links.lww.com/RLI/A863>.

Image Analysis

Image analysis was performed on a PACS (picture archiving and communication system) workstation certified for clinical use (MERLIN 7.1.22; Phönix-PACS GmbH). All 3D DESS images were assessed by 2 radiologists (G.C.F. and A.A.M.) in random order, independently and blinded to all clinical information.

Semiquantitative Measurements

Multiplanar reconstructions were used for optimal image assessment. Images were reconstructed separately for each nerve root to obtain the best possible coronal and sagittal oblique images along each nerve root, as well as standard transverse images. The dimensions of the DRG, in regard to length, width, and width/length ratio, were measured at the maximal visualization plane. The length was defined as the longitudinal distance between the proximal and distal ends of the DRG along the spinal nerve. The width was defined as the vertical distance at the midpoint perpendicular to the longitudinal axis of the DRG.²⁰

Qualitative Measurements

Cervical nerve root morphology at the neuroforaminal level was graded using a 3-point grading system with the following definitions:

- Grade 0: No discernible morphological changes; normal nerve appearance.
- Grade 1: Slight to moderate compression of the nerve root, accounting for less than 50% of the nerve diameter.
- Grade 2: Severe compression or collapse of the nerve root, involving more than 50% of the nerve diameter (Fig. 2).

Diagnostic confidence, which primarily assesses the overall diagnostic accuracy and visual impression of an image, was evaluated using a 4-point Likert scale, ranging from 1 (poor) to 4 (excellent). The signal intensity of the cervical nerve rootlets, roots, and DRG was defined as either intermediate/normal intensity or high/abnormal intensity in comparison with the signal intensity of the spinal cord. The visibility of cervical nerve rootlets, roots, and DRG was graded with a 3-point Likert-scale (1 = poor, 2 = moderate, and 3 = sharp). Image artifacts including blurring, streaking, and shading due to voluntary or involuntary movement were graded with a 4-point Likert scale (1 = severe artifacts, 2 = considerable artifacts, 3 = mild artifacts, and 4 = no artifacts).

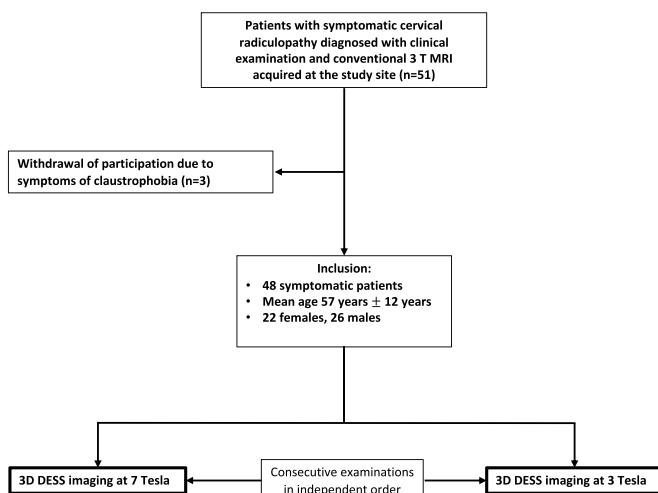


FIGURE 1. Selection flowchart for patients with symptomatic cervical radiculopathy. All included patients received a conventional 3 T MRI during the clinical workup as well as 3D dual-echo steady-state (DESS) at 7 T and at 3 T.

Downloaded from <http://onlinelibrary.wiley.com/doi/10.1002/ir.1444> by BhDMf5ePHKav1ZTEouunt1ZCN44HLHhZzgo

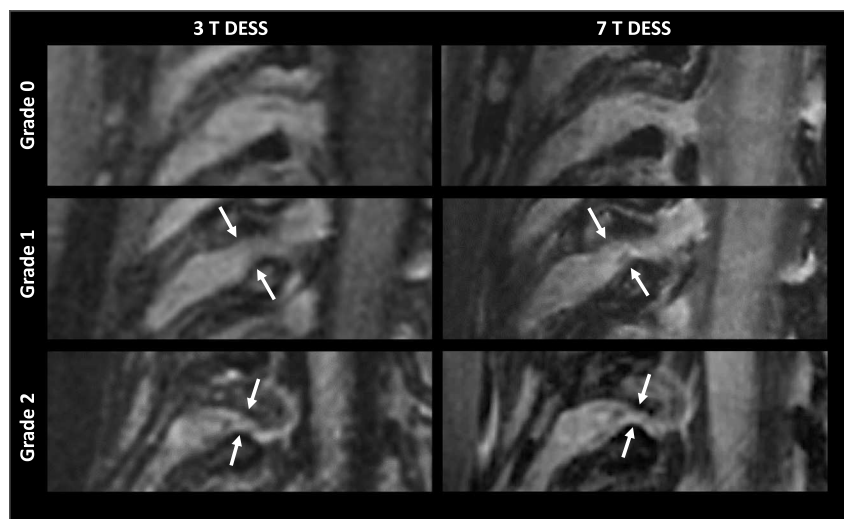


FIGURE 2. Nerve root compression grading at the level of the neuroforamen using 3D DESS MRI at 3 T and 7 T. Direct compression of cervical nerve roots was graded as follows: grade 0, no discernible morphological changes, normal nerve appearance; grade 1, slight to moderate compression of the nerve root, accounting for less than 50% of the nerve diameter (arrows); grade 2, severe compression or collapse of the nerve root, involving more than 50% of the nerve diameter (arrows). Note: Right cervical nerve roots from different patients are depicted in oblique coronal reconstructions of DESS images over the neuroforamen.

The degree of neuroforaminal stenosis was graded on the conventional 3 T MRI according to Park et al¹⁴ and divided into grade 0 to 3. The neuroforamina and nerve roots were assessed on sagittal oblique T2-weighted images for the degree of perineural fat obliteration surrounding the nerve and for morphologic changes of the nerve root, for example, compression or collapse. Grading was done as follows: grade 0 = absent stenosis, grade 1 (mild) = perineural fat obliteration under 50% of the root circumference and no morphologic changes, grade 2 (moderate) = perineural fat obliteration over 50% of the root circumference without morphologic changes of the nerve root, and grade 3 (severe) = morphological nerve root changes combined with perineural fat obliteration.

Statistics

Distribution of continuous data was assessed using the Shapiro-Wilk test. Separate binary logistic regression models were used to assess the relationship between the degree of nerve compression and the degree of neuroforaminal stenosis with the occurrence of sensory or motor dysfunction. Receiver operating characteristic curves were used to assess the diagnostic performance of the neuroforaminal stenosis grading and nerve compression grading in predicting symptoms of sensory or motor dysfunction. The Wilcoxon signed rank test was also used to compare DRG measurements and qualitative measurements between 3 T DESS and 7 T DESS MRI. Kendall τ test was used to find correlations between the signal intensities of the nerve rootlets and DRG and the degree of neuroforaminal stenosis. Interreader agreement was assessed with the intraclass correlation coefficient (ICC) for continuous variables and weighted Cohen κ for categorical variables. To assess the differences between the Cohen κ values and the ICC values, the χ^2 test and the analysis of variance were used, respectively. Statistics were performed in SPSS (v. 28.0 IBM Corp) by G.C.F. In all analyses, a $P \leq 0.05$ was considered statistically significant.

RESULTS

Forty-eight patients (mean age, 57 ± 12 years; 22 women) diagnosed with cervical radiculopathy were included into the study. In total, 672 neuroforamina were examined, and each patient was diagnosed with at least 1 moderate neuroforaminal stenosis on conventional 3 T MRI. The highest incidence of moderate to severe neuroforaminal

stenosis was observed at the C6 level ($n = 68$) followed by the C7 level ($n = 43$, Table 1). Each patient demonstrated symptoms of sensory or motor dysfunctions, which were also most commonly found at the level of C6 ($n = 38$) and C7 ($n = 23$). All patients underwent surgical decompression of at least 1 cervical nerve root. Significant improvements in NDI scores were observed postoperatively, thus confirming the success of the surgery (mean NDI preoperative: 26.6 ± 4.7 , NDI postoperative: 22.6 ± 6.5 , $P < 0.001$). No difference was found between males and females regarding the number and location of neuroforaminal stenosis ($P = 0.86$ and $P = 0.53$, respectively).

Assessment of Nerve Root Compression

Severe compression or collapse of the nerve root was observed 10 times for C4, 14 times for C5, 28 times for C6, and 18 times for C7, as determined by 7 T DESS MRI. Slight to moderate nerve root compressions were detected 2 times for C3, 10 times for C4, 18 times for C5, 38 times for C6, and 20 times for C7. Overall grading of the cervical nerve root compression did not exhibit a significant difference between 3 T and 7 T MRI (mean 3 T MRI: 1.38 ± 0.69 , mean 7 T MRI: 1.35 ± 0.67 , $P = 0.843$, Table 2). However, an overall higher diagnostic confidence was observed on 7 T MRI than on 3 T MRI ($P = 0.01$, Fig. 3). Interreader agreement for the assessment of the nerve root compression was substantial for 3 T DESS, with κ of 0.91 (95% confidence interval [CI], 0.78–0.98), and for 7 T DESS with κ of 0.92 (95% CI, 0.81–0.98; Supplementary Table S3, <http://links.lww.com/RLI/A863>). No significant difference was found between the Cohen κ scores assessed at 3 T and 7 T ($P > 0.05$).

Correlation of Neuroforaminal Stenosis Assessed on Clinical 3 T MRI and Nerve Root Compression on 7 T DESS MRI With Symptoms of Sensory or Motor Dysfunction

Compared with patients with no neuroforaminal stenosis, patients with mild and moderate stenosis (grade 1 and 2) were 9.1 (95% CI, 3.9–21.6) and 29.1 (95% CI, 12.8–66.5) times more likely to exhibit symptoms of sensory or motor dysfunction at the level of stenosis ($P < 0.01$ for linear trend, respectively). Patients with severe neuroforaminal stenosis (grade 3) were 31.3 (95% CI, 13.1–75.3) times

more likely to exhibit symptoms of sensory or motor dysfunction at the level of stenosis. Assessment of the direct nerve root compression on 7 T DESS MRI revealed that patients with slight to moderate compression and severe compression were 22.7 (95% CI, 9.9–51.9) and 48.4 (95% CI, 21.5–74.2) times more likely to exhibit symptoms of sensory or motor dysfunction at the level of stenosis, compared with patients with no nerve compression ($P < 0.01$ for linear trend, respectively).

The receiver operating characteristic analysis showed a good performance in predicting symptoms of sensory or motor dysfunction assessing the neuroforaminal stenosis with the Park et al¹⁴ classification (area under the curve [AUC], 0.84). However, the performance of severe grade 3 stenosis alone in predicting symptoms of sensory or motor dysfunction was notably lower (AUC, 0.63). An overall better performance was achieved by combining the assessment of neuroforaminal stenosis according to Park et al¹⁴ with the assessment of direct nerve compression (AUC, 0.87).

To calculate sensitivity and specificity, the MRI-based scores were dichotomized into 2 variables: foramen stenosis and/or nerve compression and foramen stenosis alone. Finally, the χ^2 test demonstrated a higher sensitivity and specificity for the combined assessment of the neuroforaminal stenosis and nerve compression than the assessment of the neuroforaminal stenosis alone (combined assessment: sensitivity, 82.9%; specificity, 90.8%; positive predictive value, 73.9%; negative predictive value, 94.4% vs neuroforaminal stenosis alone: sensitivity, 65.9%; specificity, 86.4%; positive predictive value, 66.7%; negative predictive value, 89.3%).

Dimensions of DRG

Measurements of the length (range of means: 6.49 ± 1.54 mm to 8.66 ± 1.93 mm), width (range of means: 4.95 ± 1.30 mm to 6.33 ± 1.24 mm), and width-to-length ratio of the DRG done on 7 T MRI and 3 T MRI were comparable, with no significant difference ($P = 0.089–0.813$; Table 3, Fig. 4). The interreader agreement for the measurements of DRG was substantial to almost perfect and was not rated significantly different between 3 T and 7 T ($P > 0.05$; ICC range [95% CI], 0.82 [0.77–0.92] to 0.97 [0.94–0.98]; Table 4).

Qualitative Assessments

The overall visibility of cervical nerve rootlets, roots, and DRG was rated significantly higher on 7 T MRI than on 3 T MRI ($P = 0.008$, Fig. 5). No significant difference in image artifacts was detected on 3 T MRI compared with 7 T MRI ($P = 0.990$). A focal high signal intensity of the cervical nerve rootlets was found in 7 cases at 3 T MRI and 5 cases at 7 T MRI. However, no significant correlation

between the degree of neuroforaminal stenosis and signal intensity of the cervical nerves was found ($P > 0.05$, Fig. 6). Interreader reliability for qualitative assessments was substantial with not significant difference between 3 T and 7 T ($P > 0.05$, Cohen κ range [95% CI], 0.86 [0.81–0.94] to 0.92 [0.87–0.97]; Supplementary Table S3, <http://links.lww.com/RLI/A863>).

DISCUSSION

In this prospective study, a total of 48 patients presenting with cervical radiculopathy underwent assessment of 3-dimensional DESS MRI scans acquired at 3 T and 7 T that provided a direct visualization of cervical nerve root compression. This approach demonstrated improved performance in predicting symptoms of sensory and motor dysfunctions, compared with the conventional grading of neuroforaminal stenosis. By combining the assessment of neuroforaminal stenosis with the direct evaluation of nerve root compression, a larger AUC was achieved, opening the possibility of a more sensitive assessment of radiculopathy in clinical routine. No significant differences between the 3 T DESS and 7 T DESS MRI in regard to the ratings of nerve root compression or the measurements of length and width in the cervical DRG were exhibited. However, the 7 T MRI scans presented significantly enhanced visualization of the cervical nerve rootlets, roots, and DRG ($P < 0.01$), along with higher diagnostic confidence ($P = 0.01$).

Three-dimensional DESS MRI was originally designed for high-resolution cartilage imaging.^{5,21,22} However, several recent studies have successfully implemented 3D DESS imaging for the visualization of nerve tissues, in particular peripheral nerves in the maxillofacial region.^{23–25} Because of its optimized contrast between fluid and adjacent structures, it is suitable for imaging of subtle nerve structures. In a study by Wang et al,¹⁵ the authors were able to demonstrate that 3D DESS sequences are superior to multiecho data image combination and 3D sampling perfection with application-optimized contrast using different flip angle evolutions sequences when assessing cervical nerve roots at 3 T MRI. Furthermore, Galley et al⁹ applied 3D DESS sequences for imaging of the cervical spine at 7 T. Thanks to the increased spatial resolution, the authors were able to identify more cervical nerve rootlets on 7 T MRI than on 3 T MRI in 21 patients, thus indicating that a higher magnetic field strength might increase diagnostic accuracy and performance. However, they solely focused on the identification of the proximal nerve rootlets, and no pathologies of the nerve rootlets were found in their study population.

In this study, we investigated a larger cohort of patients with cervical radiculopathy, many of whom exhibited severe neuroforaminal stenosis. Our findings revealed a significantly improved visibility of

TABLE 2. Comparison of Qualitative Assessments of the Cervical Nerve Rootlets, Roots, and Dorsal Root Ganglia Measured at 7 T and 3 T DESS MRI

	7 T DESS	3 T DESS	P
Image artifacts* [†]	3.25 ± 0.26	3.26 ± 0.21	0.990
Visibility of nerve rootlets, roots, and dorsal root ganglia* [‡]	2.49 ± 0.16	2.27 ± 0.24	0.008
Overall diagnostic confidence* [§]	3.24 ± 0.15	3.01 ± 0.58	0.010
Nerve root compression*	1.35 ± 0.67	1.38 ± 0.69	0.843

*Data are given as mean ± standard deviation.

[†]Measured on a 5-point Likert scale: 1 = severe artifacts, 2 = considerable artifacts, 3 = mild artifacts, and 4 = no artifacts.

[‡]Measured on a 3-point Likert scale: 1 = poor, 2 = moderate, and 3 = sharp.

[§]Measured on a 4-point Likert scale: 1 = poor, 2 = fair, 3 = good, and 4 = excellent.

^{||}Measured on a 3-point Likert scale: 1 = normal/no changes, 2 = slight to moderate compression, and 3 = severe compression or collapse of the cervical nerve root.

DESS, dual-echo steady-state; MRI, magnetic resonance imaging.

Downloaded from <http://online.lww.com/InvestigativeRadiology> by BnDmIsePhKav12Eoutm10In14a4kL1Ez0p sIH04XMI0h0yWC0X1AMWYQpI1lCHD313D00dRfY7T75F4C8VCl1Y0abgGZQZdGj2MwZLel= on 10/27/2023

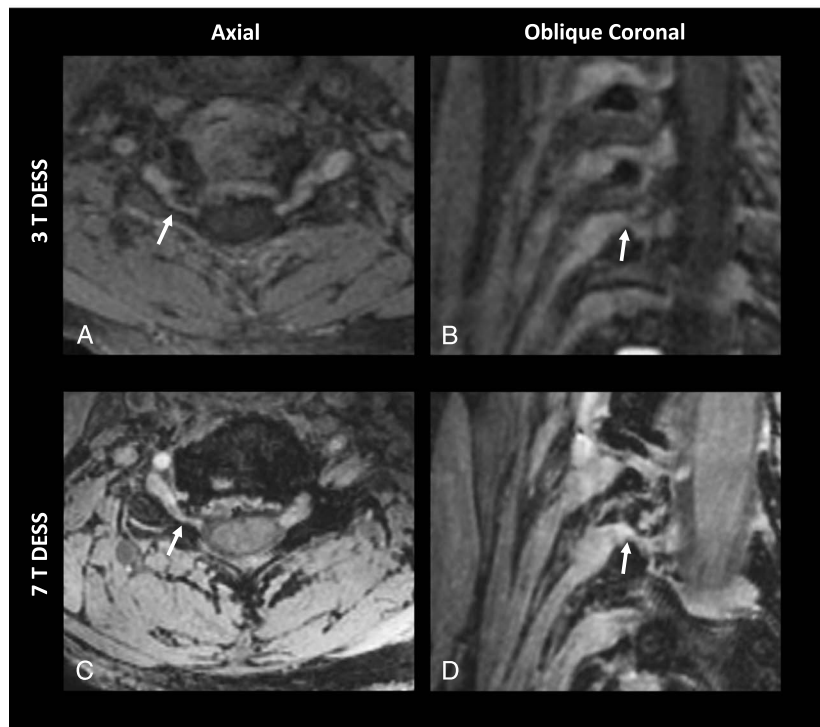


FIGURE 3. Multiplanar 3D DESS MRI scans of a patient with surgically confirmed neuroforaminal stenosis at the level of C7 on the right side. Multiplanar reformations of the 3D DESS sequence on 3 T MRI (A and B) and 7 T MRI (C and D) directly visualize the compressed cervical nerve root at the level of stenosis (arrows). Note the improved visibility of the nerve root on the 3D DESS images acquired at 7 T.

nerve rootlets, roots, and DRG at 7 T DESS compared with 3 T DESS. Notably, unlike conventional MRI, direct visualization and assessment of cervical nerve root compression in cases of severe neuroforaminal stenosis was feasible, and both raters demonstrated a higher level of diagnostic confidence for 7 T MRI.

When using the classification system by Park et al,¹⁴ morphological changes in the nerve roots along with perineural fat obliteration are consistently graded as severe stenosis. However, our study demonstrated that direct assessment of nerve root compression using 7 T DESS allows for a more sensitive grading and was able to improve the performance in predicting symptoms of sensory or motor dysfunction.

In addition, the enhanced visibility of nerve rootlets and DRG holds significant value in cases involving traumatic lesions, such as those affecting the brachial plexus. Accurate differentiation between

preganglionic and postganglionic injuries is vital for appropriate treatment, but conventional MRI often yields inconclusive results in visualizing root avulsion.^{26–29} Therefore, 3D DESS imaging at higher magnetic field strengths might add a potential benefit over imaging at lower magnetic field strengths when assessing traumatic nerve lesions.

In this study, we also investigated the signal intensity of cervical nerve rootlets, roots, and DRG in patients with radiculopathy due to severe neuroforaminal stenosis. We hypothesized that imaging at 7 T might provide a slight signal increase of the impinged nerves due to swelling. However, no statistical correlation between an increased signal intensity of the nerve rootlets, roots, and DRG and the degree of neuroforaminal stenosis was detected. We concluded that some of the observed signal increase of nerve rootlets and DRG at the neuroforaminal level likely have other causes, such as the altered velocity of the cerebrospinal fluid (CSF).

TABLE 3. Comparison of Mean Measurements of the Cervical DRG Between 7 T DESS and 3 T DESS MRI

DRG	7 T DESS			3 T DESS			P
	Length, mm*	Width, mm*	Width/Length Ratio	Length, mm*	Width, mm*	Width/Length Ratio	
C2	6.64 ± 1.54	5.24 ± 1.21	0.79	6.49 ± 1.54	5.19 ± 1.21	0.79	0.089
C3	6.91 ± 1.79	5.15 ± 1.17	0.76	6.90 ± 1.77	5.16 ± 1.14	0.76	0.475
C4	6.66 ± 1.83	4.95 ± 1.30	0.75	6.68 ± 1.79	4.97 ± 1.27	0.76	0.813
C5	7.59 ± 1.90	5.53 ± 1.43	0.73	7.54 ± 1.88	5.52 ± 2.39	0.74	0.489
C6	8.10 ± 1.87	6.11 ± 1.22	0.76	8.05 ± 1.87	6.11 ± 1.19	0.77	0.225
C7	8.50 ± 1.87	6.33 ± 1.24	0.75	8.47 ± 1.85	6.33 ± 1.22	0.76	0.530
C8	8.66 ± 1.93	6.30 ± 1.12	0.74	8.61 ± 1.94	6.29 ± 1.01	0.75	0.132

*Mean ± standard deviation;

DRG, dorsal root ganglia; DESS, dual-echo steady-state.

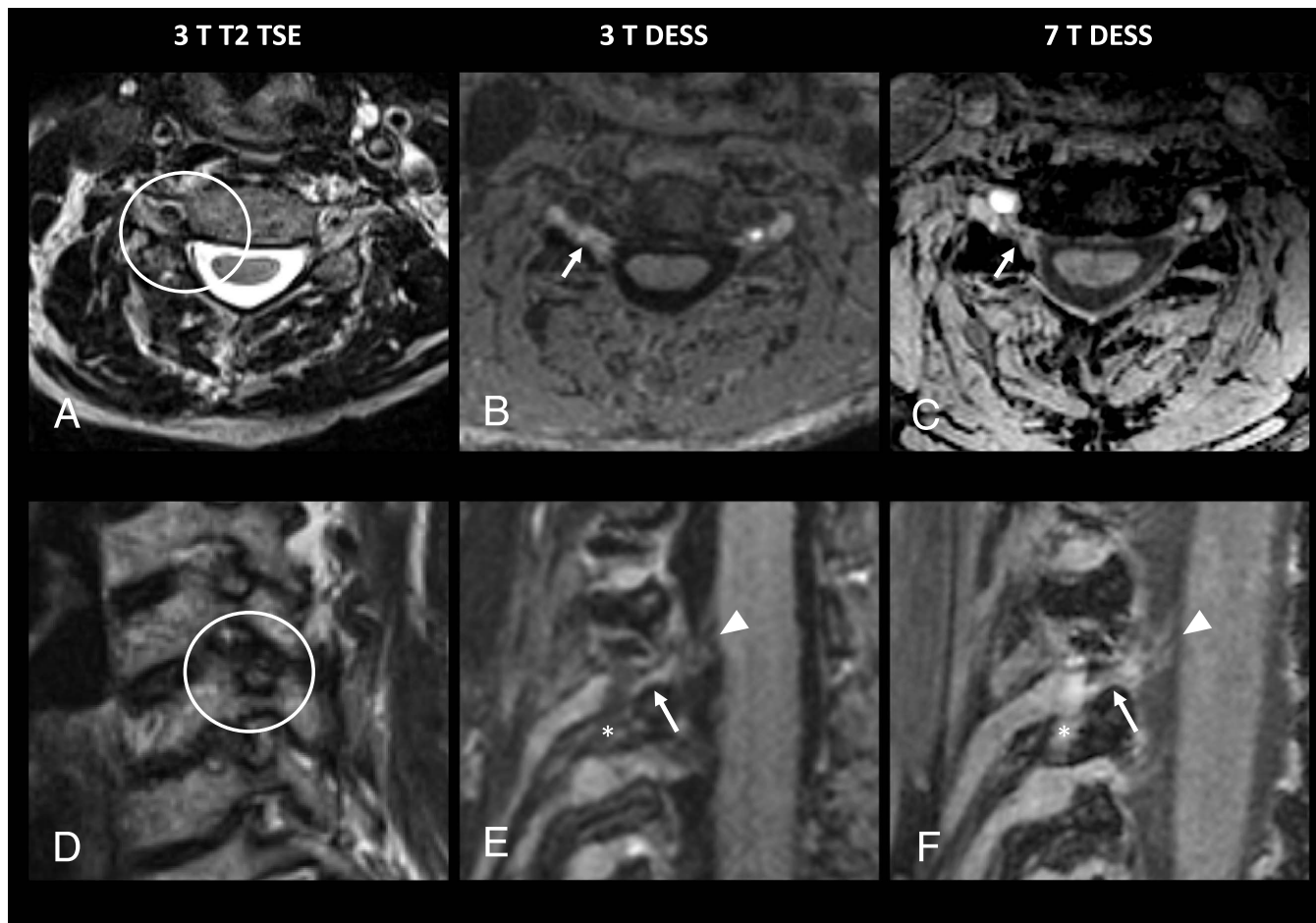


FIGURE 4. Multiplanar MRI scans of a patient with symptomatic cervical radiculopathy at the level of C6 of the right side. A and D, Images show a severe neuroforaminal stenosis on axial and oblique sagittal oblique conventional 3 T T2-weighted TSE images (circle). Multiplanar reformations of a 3D DESS sequence at 3 T (B and E) and 7 T (C and F) directly visualize the compressed cervical nerve root at the level of stenosis (arrows) as well as the attached cervical nerve rootlets (arrowhead). The asterisks are pointing on a partial overlay due to a cervical vein. TSE, turbo-spin echo.

Because of the T2 weighting part of the DESS sequence image contrast, fluids with low flow or stationary fluids appear bright as it is the case, for example, with intra-articular fluid. In contrast, the faster moving CSF around the spine cord appeared dark on the DESS images at 3 T MRI

and 7 T MRI. In a previous study, Galley et al⁹ described an increased fluid signal around the vermillion and pericerebellar cisterns, which the authors also attributed to altered CSF flow velocities. Therefore, we hypothesized that stenosis of the neuroforamen might reduce the motion of the CSF, thus causing a hyperintense signal around the nerve rather than the nerve itself. However, the distinction between nerve root edema and fluid artifacts should be evaluated in future studies.

TABLE 4. Interreader Agreement for the Measurements of the DRG on the 3D DESS Images at 7 T and 3 T DESS MRI

DRG	Interreader Agreement for Rater 1 and 2*	
	7 T DESS	3 T DESS
C2	0.89 [0.82–0.94]	0.83 [0.60–0.93]
C3	0.82 [0.77–0.92]	0.95 [0.90–0.97]
C4	0.87 [0.74–0.94]	0.87 [0.77–0.93]
C5	0.92 [0.80–0.97]	0.95 [0.91–0.98]
C6	0.89 [0.81–0.96]	0.97 [0.94–0.98]
C7	0.94 [0.89–0.99]	0.88 [0.75–0.93]
C8	0.93 [0.85–0.96]	0.92 [0.87–0.96]

*Interclass correlation coefficient; data are given with 95% confidence interval.

DRG, dorsal root ganglia; DESS, dual-echo steady-state.

There are certain limitations of this study. Ultra-high field MRI at 7 T still is not widely available, which limits the general applicability. Only the 3D DESS sequence was acquired at 7 T. In general, a variety of sequences are available at 7 T. However, in this study, we focused on direct nerve visualization and assessment, for which the 3D DESS sequence provides higher sensitivity and specificity. To ensure comparable results obtained with state-of-the-art imaging equipment in a “normal” clinical workflow, no additional adjustments or corrections, such as bias field corrections, were made beyond the scanner’s “standard” prescan in “clinical” mode, and no pTx techniques were used. In addition, the water excitation option of the DESS sequence at 7 T is only available for nonselective RF pulse excitation, which may result in the need for greater coverage and/or more slice oversampling than would be required at 3 T with slab-selective water excitation. In this study, the difference in coverage along the slice encoding direction was primarily determined by the respective number of slices and slice oversampling steps allowed by the software versions on the consoles.

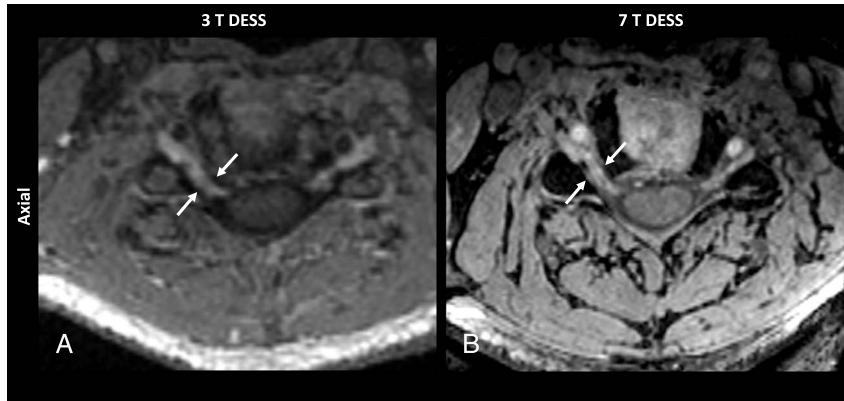


FIGURE 5. Axial reformations of a 3D DESS sequence of a patient with symptomatic cervical radiculopathy at the level of the right C5 nerve root, acquired at 3 T MRI (A) and 7 T MRI (B). Note the increased spatial resolution with better visualization of the cervical nerve root at 7 T MRI compared with 3 T MRI (arrows).

Direct intraoperative confirmation of the degree of stenosis was not possible due to the different surgical approaches used by the spine surgeons. Preoperative diagnosis of neuroforaminal stenosis was made by the surgeons on the basis of symptoms, physical and clinical examination, and the results of conventional clinical 3 T MRI, and no other tests, such as electrophysiological tests, were available at the time of enrolment. Furthermore, only patients with radiculopathy due to

degenerative changes were included in this study so the possible role of 7 T MRI for traumatic avulsions of cervical nerve roots could not be assessed.

In summary, 3D DESS MRI at 7 T provides reliable assessment of cervical nerve rootlets, roots, and DRG in patients diagnosed with cervical radiculopathy with higher image quality and diagnostic confidence than in 3 T MRI.

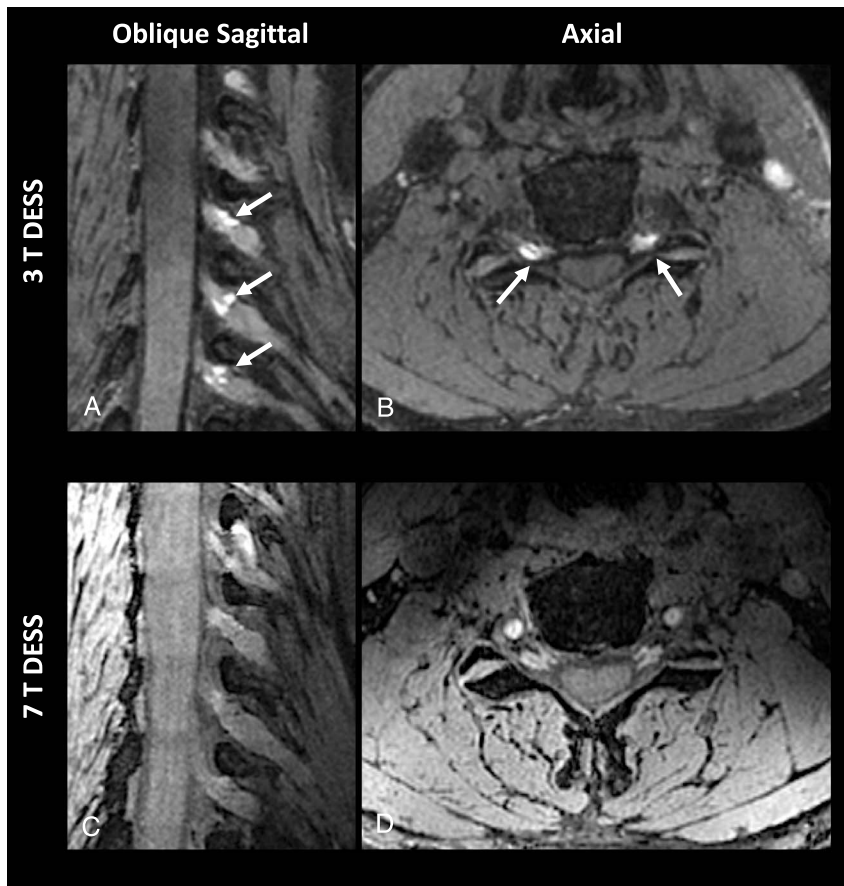


FIGURE 6. Oblique sagittal and axial reformations of a 3D DESS sequence of the cervical spine acquired at 3 T MRI (A and B) as well as on 7 T MRI (C and D). Note that the 3 T MRI is more susceptible to the low velocity of the CSF at the level of the neuroforaminal recesses resulting in a focal signal increase and reduced accessibility of the cervical nerve root (arrows) compared with 7 T MRI. CSF, cerebrospinal fluid.

Downloaded from http://journals.lww.com/investigativeradiology by 54.159.145.12 on 10/27/2023

Key Results

- Direct assessment of the cervical nerve root compression was feasible on 3 and 7 T DESS MRI scans, with C6 and C7 being the most affected nerve roots (severe compression, C6 n = 20 and C7 n = 18).
- Diagnostic confidence as well as the visibility of cervical nerve rootlets, roots, and DRG were rated significantly higher on 7 T DESS MRI than on 3 T DESS MRI (diagnostic confidence: $P = 0.01$, visibility: $P < 0.01$).
- Assessment of nerve root compression at 7 T DESS improved the performance in predicting sensory or motor dysfunction over the assessment of neuroforaminal stenosis alone (AUC combined: 0.87).

ACKNOWLEDGMENTS

The authors thank Sabine Schrimpf for critical proofreading and language editing. Imaging was performed with support of the Swiss Center for Musculoskeletal Imaging, SCMI, Balgrist Campus AG, Zurich.

REFERENCES

- Pazahr S, Nanz D, Sutter R. 7 T musculoskeletal MRI: fundamentals and clinical implementation. *Invest Radiol*. 2023;58:88–98.
- Aringhieri G, Zampa V, Tosetti M. Musculoskeletal MRI at 7 T: do we need more or is it more than enough? *Eur Radiol Exp*. 2020;4:48.
- Runge VM, Heverhagen JT. The clinical utility of magnetic resonance imaging according to field strength, specifically addressing the breadth of current state-of-the-art systems, which include 0.55 T, 1.5 T, 3 T, and 7 T. *Invest Radiol*. 2022;57:1–12.
- Eisenhut F, Schläpfer SM, Hock S, et al. Ultra-high-field 7 T magnetic resonance imaging including dynamic and static contrast-enhanced T1-weighted imaging improves detection of secreting pituitary microadenomas. *Invest Radiol*. 2022;57:567–574.
- Germann C, Galley J, Falkowski AL, et al. Ultra-high resolution 3D MRI for chondrocalcinosis detection in the knee—a prospective diagnostic accuracy study comparing 7-Tesla and 3-Tesla MRI with CT. *Eur Radiol*. 2021;31:9436–9445.
- Lazik-Palm A, Kraff O, Johst S, et al. Morphological and quantitative 7 T MRI of hip cartilage transplants in comparison to 3 T-initial experiences. *Invest Radiol*. 2016;51:552–559.
- Treutlein C, Bäuerle T, Nagel AM, et al. Comprehensive assessment of knee joint synovitis at 7T MRI using contrast-enhanced and non-enhanced sequences. *BMC Musculoskelet Disord*. 2020;21:116.
- Heiss R, Weber MA, Balbach E, et al. Clinical application of ultrahigh-field-strength wrist MRI: a multireader 3-T and 7-T comparison study. *Radiology*. 2023;307:e220753.
- Galley J, Sutter R, Germann C, et al. High-resolution in vivo MR imaging of intraspinal cervical nerve rootlets at 3 and 7 Tesla. *Eur Radiol*. 2021;31:4625–4633.
- Gast LV, Baier LM, Meixner CR, et al. MRI of potassium and sodium enables comprehensive analysis of ion perturbations in skeletal muscle tissue after eccentric exercise. *Invest Radiol*. 2023;58:265–272.
- Riegler G, Drlicek G, Kronnerwetter C, et al. High-resolution axonal bundle (fascicle) assessment and triple-echo steady-state T2 mapping of the median nerve at 7 T: preliminary experience. *Invest Radiol*. 2016;51:529–535.
- Caridi JM, Pumberger M, Hughes AP. Cervical radiculopathy: a review. *HSS J*. 2011;7:265–272.
- Kang KC, Lee HS, Lee JH. Cervical radiculopathy focus on characteristics and differential diagnosis. *Asian Spine J*. 2020;14:921–930.
- Park HJ, Kim SS, Lee SY, et al. A practical MRI grading system for cervical foraminal stenosis based on oblique sagittal images. *Br J Radiol*. 2013;86:20120515.
- Wang Q, Li H, Kong J, et al. Diagnostic agreement between 3.0-T MRI sequences of nerve root and surgery in patients with cervical radiculopathy: a retrospective study. *Medicine (Baltimore)*. 2021;100:e24207.
- Tawa N, Rhoda A, Diener I. Accuracy of magnetic resonance imaging in detecting lumbo-sacral nerve root compromise: a systematic literature review. *BMC Musculoskelet Disord*. 2016;17:386.
- Bakhtadze MA, Vernon H, Zakharova OB, et al. The Neck Disability Index-Russian language version (NDI-RU): a study of validity and reliability. *Spine (Phila Pa 1976)*. 2015;40:1115–1121.
- Khan I, Sivaganesan A, Archer KR, et al. Does Neck Disability Index correlate with 12-month satisfaction after elective surgery for cervical radiculopathy? Results from a National Spine Registry. *Neurosurgery*. 2020;86:736–741.
- Young IA, Dunning J, Butts R, et al. Reliability, construct validity, and responsiveness of the Neck Disability Index and numeric pain rating scale in patients with mechanical neck pain without upper extremity symptoms. *Physiother Theory Pract*. 2019;35:1328–1335.
- Shen J, Wang HY, Chen JY, et al. Morphologic analysis of normal human lumbar dorsal root ganglion by 3D MR imaging. *AJNR Am J Neuroradiol*. 2006;27:2098–2103.
- Kohl S, Meier S, Ahmad SS, et al. Accuracy of cartilage-specific 3-Tesla 3D-DESS magnetic resonance imaging in the diagnosis of chondral lesions: comparison with knee arthroscopy. *J Orthop Surg Res*. 2015;10:191.
- Gersing AS, Schwaiger BJ, Heilmeyer U, et al. Evaluation of chondrocalcinosis and associated knee joint degeneration using MR imaging: data from the osteoarthritis initiative. *Eur Radiol*. 2017;27:2497–2506.
- Kim Y, Jeong HS, Kim HJ, et al. Three-dimensional double-echo steady-state with water excitation magnetic resonance imaging to localize the intraparotid facial nerve in patients with deep-seated parotid tumors. *Neuroradiology*. 2021;63:731–739.
- Burian E, Sollmann N, Ritschl LM, et al. High resolution MRI for quantitative assessment of inferior alveolar nerve impairment in course of mandible fractures: an imaging feasibility study. *Sci Rep*. 2020;10:11566.
- Al-Haj Husain A, Solomons M, Stadlinger B, et al. Visualization of the inferior alveolar nerve and lingual nerve using MRI in oral and maxillofacial surgery: a systematic review. *Diagnostics (Basel)*. 2021;11:1657.
- Shin AY, Spinner RJ, Steinmann SP, et al. Adult traumatic brachial plexus injuries. *J Am Acad Orthop Surg*. 2005;13:382–396.
- Terzis JK, Kostopoulos VK. The surgical treatment of brachial plexus injuries in adults. *Plast Reconstr Surg*. 2007;119:73e–92e.
- Yoshikawa T, Hayashi N, Yamamoto S, et al. Brachial plexus injury: clinical manifestations, conventional imaging findings, and the latest imaging techniques. *Radiographics*. 2006;26(Suppl 1):S133–S143.
- Wade RG, Takwoingi Y, Wormald JCR, et al. MRI for detecting root avulsions in traumatic adult brachial plexus injuries: a systematic review and meta-analysis of diagnostic accuracy. *Radiology*. 2019;293:125–133.